

Plant Communications, Volume 2

Supplemental information

**NLR immune receptor RB is differentially targeted by two homologous
but functionally distinct effector proteins**

Jinping Zhao and Junqi Song

1 **Supplemental Information**

2 **NLR Immune Receptor RB Is Differentially Targeted by Two Homologous but**
3 **Functionally Distinct Effector Proteins**

4

5 **Jinping Zhao¹ and Junqi Song^{1,2*}**

6 ¹Texas A&M AgriLife Research Center at Dallas, Dallas, Texas 75252, USA

7 ²Department of Plant Pathology and Microbiology, Texas A&M University, College Station,
8 Texas 77843, USA

9

10

11

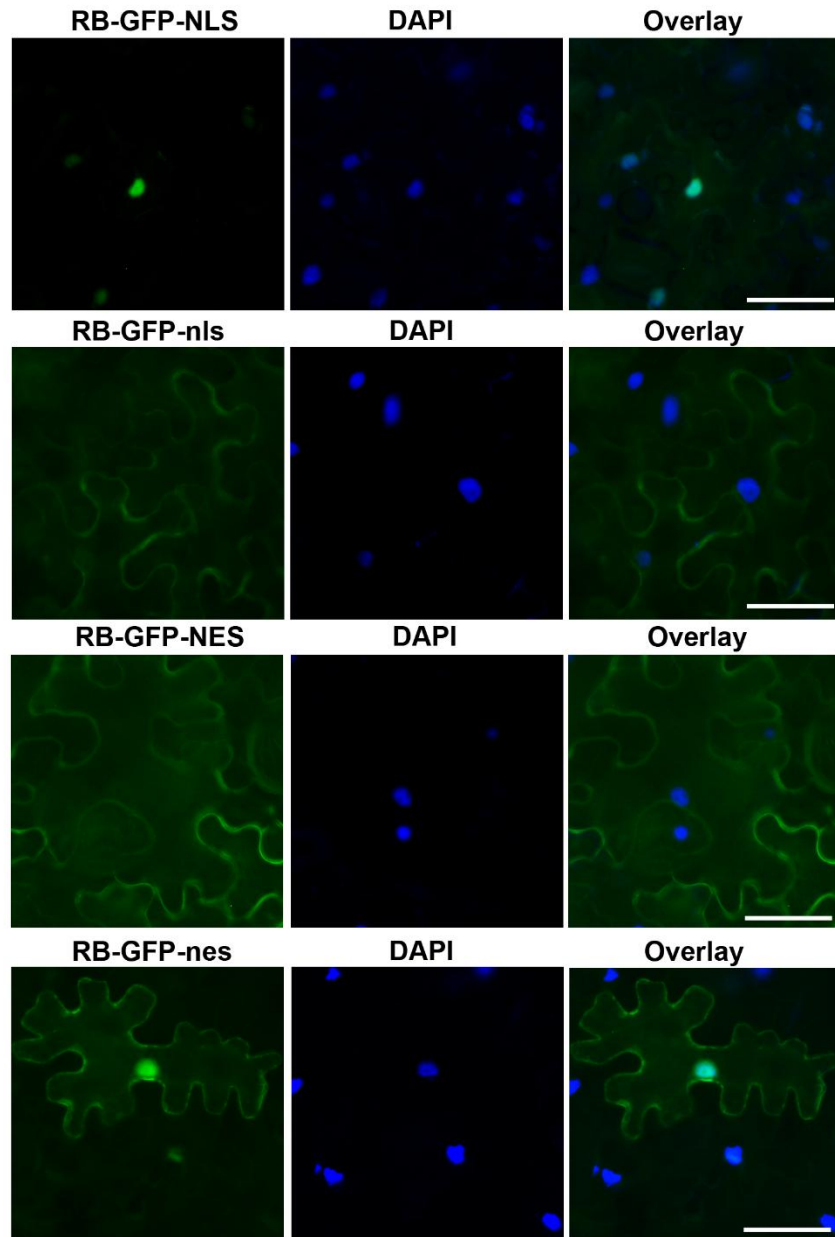
12

13

14

15

16

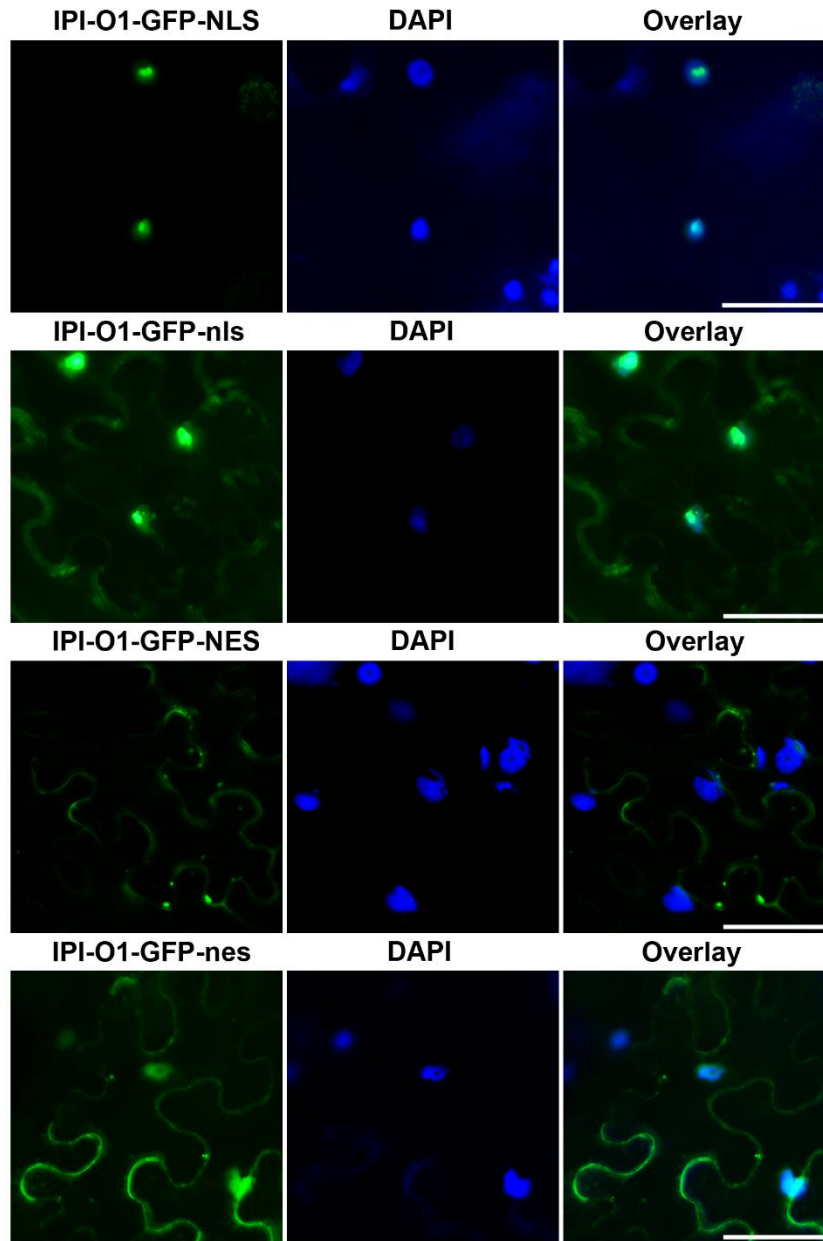


17

18 **Supplemental Figure 1. Microscopic Analysis of Subcellular Localization of RB Fusion**
 19 **Proteins.**

20 Microscopic analysis of subcellular localization of RB fusion proteins. RB constructs carrying a
 21 C-terminal GFP tag together with WT or mutated nuclear localization signal (NLS/nls) or
 22 nuclear export signal (NES/nes) were expressed in *N. benthamiana*, and subcellular localization
 23 was determined at 48 hpi (left). DAPI staining depicts nuclei in blue (middle). An overlay of

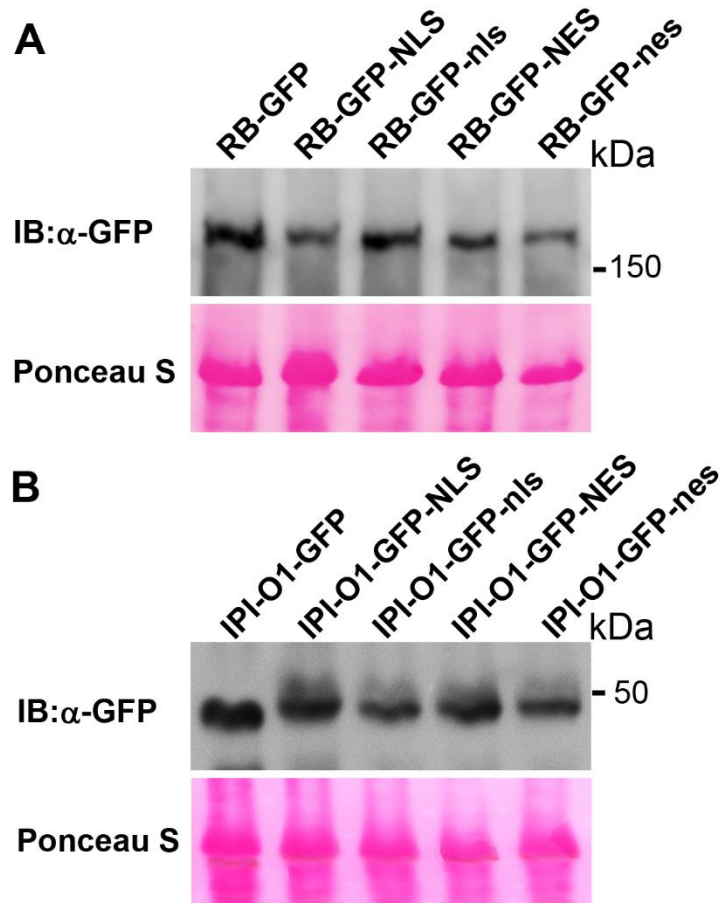
24 GFP and DAPI fluorescence signals is shown on the right. Scale bars represent 50 μm . The
25 experiments were repeated three times with similar results.



26

27 **Supplemental Figure 2. Microscopic Analysis of Subcellular Localization of IPI-O1 Fusion**
 28 **Proteins.**

29 Microscopic analysis of subcellular localization of IPI-O1 fusion proteins. IPI-O1 constructs
 30 carrying a C-terminal GFP tag and WT or mutated NLS/nls or NES/nes were expressed in *N.*
 31 *benthamiana*, and subcellular localization was determined at 48 hpi (left). DAPI staining depicts
 32 nuclei in blue (middle). An overlay of GFP and DAPI fluorescence signals is shown on the right.
 33 Scale bars represent 50 μ m. The experiments were repeated three times with similar results.



35

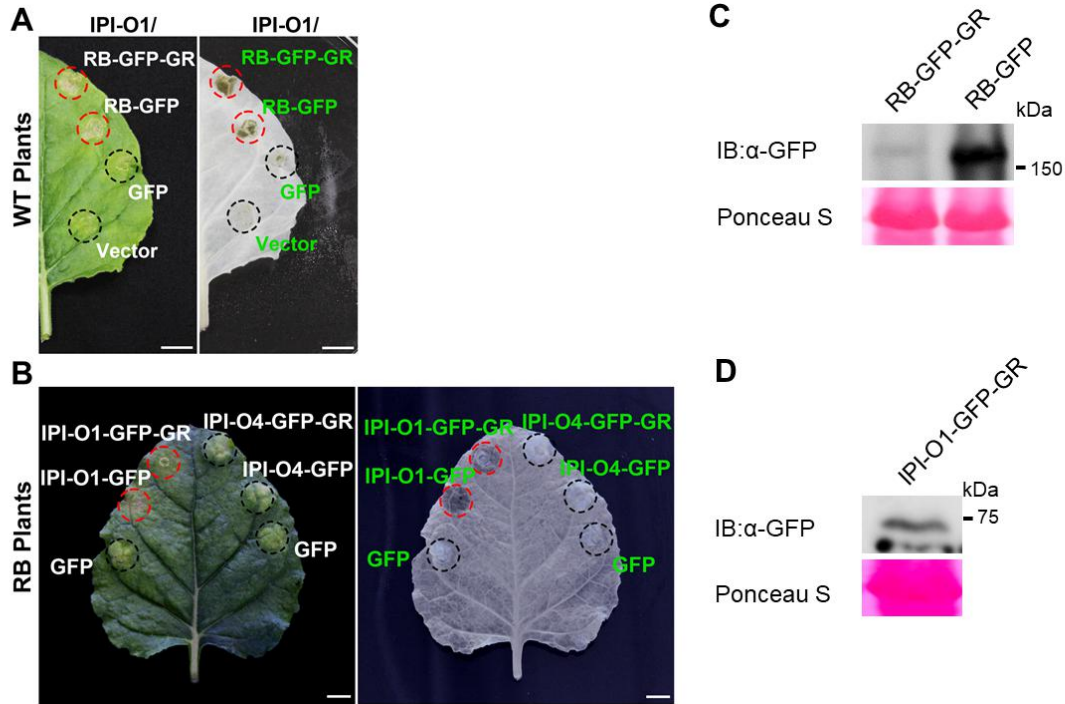
36 **Supplemental Figure 3. Western Blot Detection of the RB and IPI-O1 Fusion Proteins with**
 37 **a WT or Mutated Nuclear Localization Signal (NLS/nls) or Nuclear Export Signal**
 38 **(NES/nes).**

39 The fusion proteins were extracted from leaves collected at 36 hpi and detected by Western
 40 blotting with an anti-GFP antibody. Ponceau S staining of immunoblots served as loading
 41 controls.

42

43

44

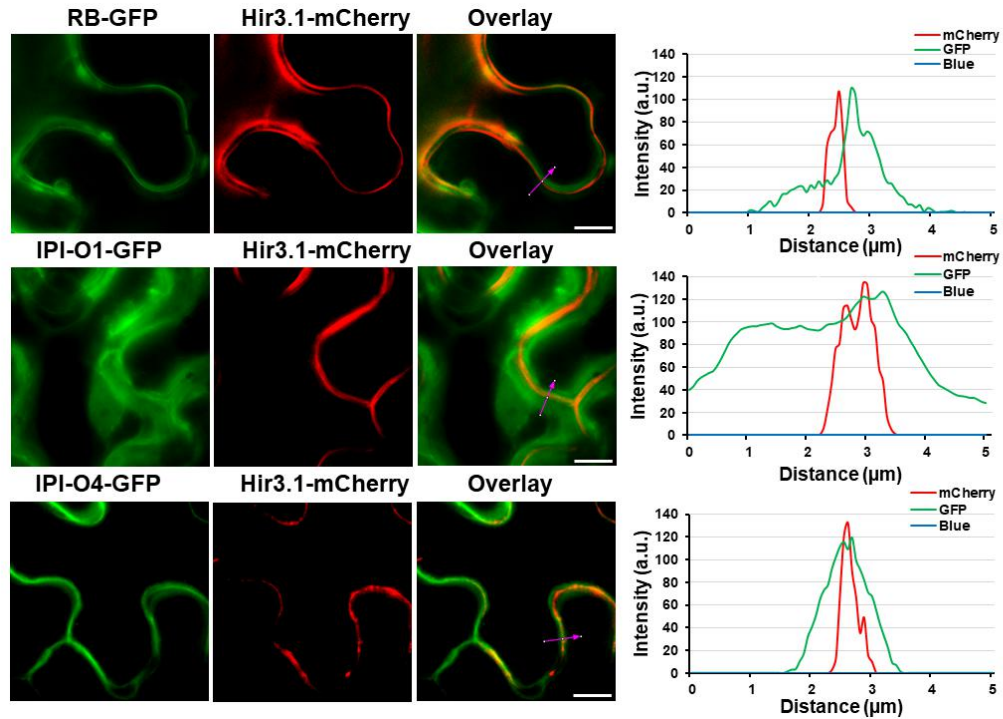


45

46 **Supplemental Figure 4. RB and IPI-O1 Trigger Cell Death in the Cytoplasm.**

47 (A) Cell death mediated by RB-GFP-GR in the presence of Myc-IPI-O1. The indicated
 48 constructs were co-expressed with IPI-O1 in *N. benthamiana*. (B) Cell death induced by IPI-O1-
 49 GFP-GR or IPI-O4-GFP-GR. The indicated constructs were each expressed in the *RB* transgenic
 50 *N. benthamiana*. Cell death induced at 48 hpi was visualized before (left) and after ethanol
 51 destaining (right). Infiltrated area is shown by a black circle and HR by a red circle. Scale bars
 52 represent 1 cm. The experiments were repeated six times with similar results. (C, D) Western
 53 blot detection of the RB (C) and IPI-O1 (D) fusion proteins with a GR tag. The fusion proteins
 54 were extracted from leaves collected at 36 hpi and detected by Western blotting with an anti-
 55 GFP antibody. Ponceau S staining of immunoblots served as loading controls.

56



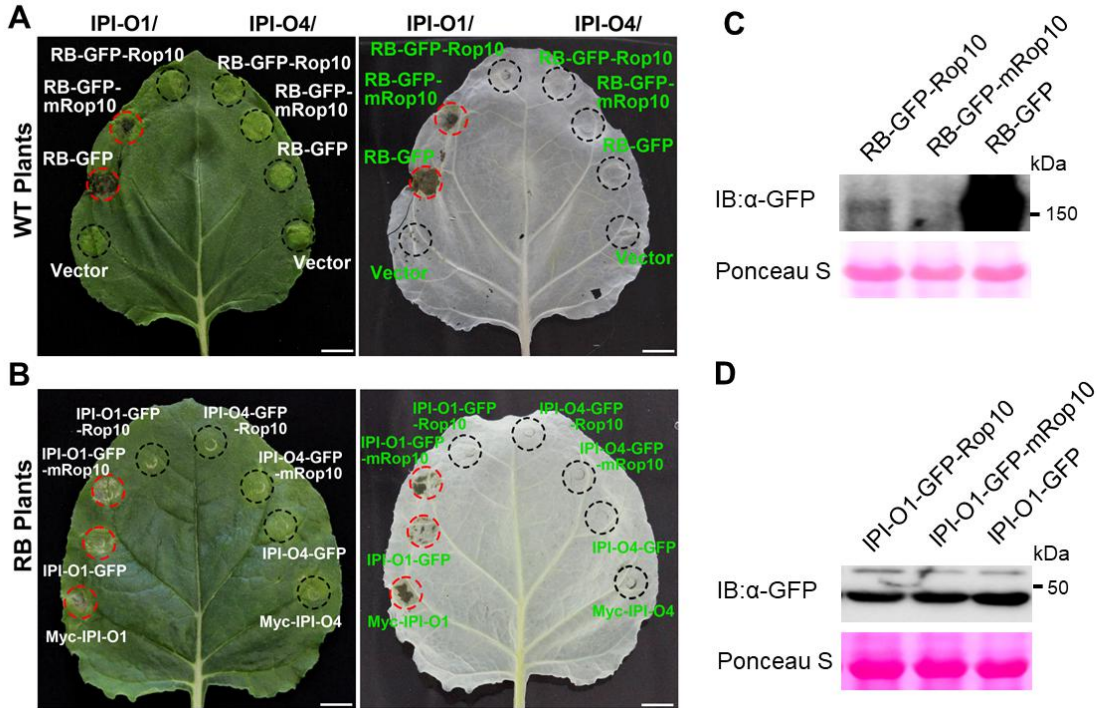
57

58 **Supplemental Figure 5. IPI-O1 and IPI-O4 but not RB Are Partially Localized to the**
 59 **Plasma Membrane.**

60 RB, IPI-O1, or IPI-O4 fused to GFP at the C-terminus was each co-expressed with the plasma
 61 membrane-localized Hir3.1-mCherry in *N. benthamiana*. Confocal images were taken at 48 hpi
 62 (left). The mCherry depicts plasma membrane in red (middle). An overlay of GFP and mCherry
 63 fluorescence signals is shown on the right. Scale bars represent 10 μm. Fluorescence intensity
 64 profiles of the GFP and mCherry channels along the direction of the arrows are shown in the
 65 plots. The experiments were repeated three times with similar results.

66

67



68

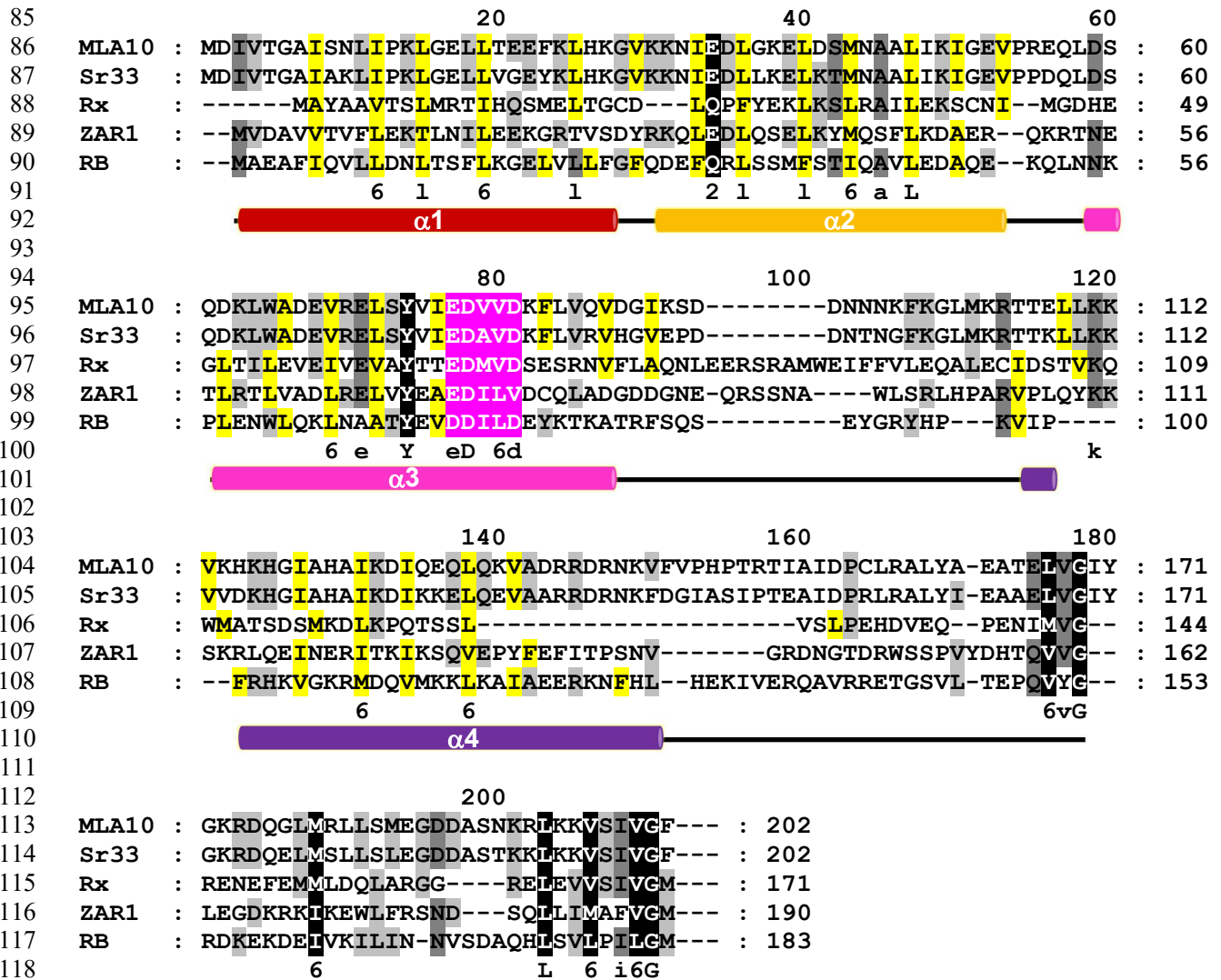
69 **Supplemental Figure 6. Membrane-Associated RB and IPI-O1 Are Unable to Induce Cell**
 70 **Death.**

71 (A) Membrane-associated RB failed to mediate cell death in the presence of IPI-O1. RB-GFP
 72 fused to Rop10 or mRop10, or RB-GFP alone was co-expressed in *N. benthamiana* with Myc-
 73 IPI-O1 or Myc-IPI-O4. (B) Membrane-associated IPI-O1 failed to induce cell death in *RB*
 74 transgenic *N. benthamiana* plants. IPI-O1 or IPI-O4 fused to Rop10 or mRop10 were each
 75 expressed in the *RB* transgenic *N. benthamiana* plants. Cell death induced at 48 hpi was
 76 visualized before and after ethanol destaining. Infiltrated area is shown by a black circle and HR
 77 by a red circle. Scale bars represent 1 cm. The experiments were repeated six times with similar
 78 results. (C, D) Western blot detection of RB (C) and IPI-O1 (D) fused to a Rop10 or mRop10 tag.
 79 The fusion proteins were extracted from leaves collected at 36 hpi and detected by Western
 80 blotting with an anti-GFP antibody. Ponceau S staining of immunoblots served as loading
 81 controls.

82

83

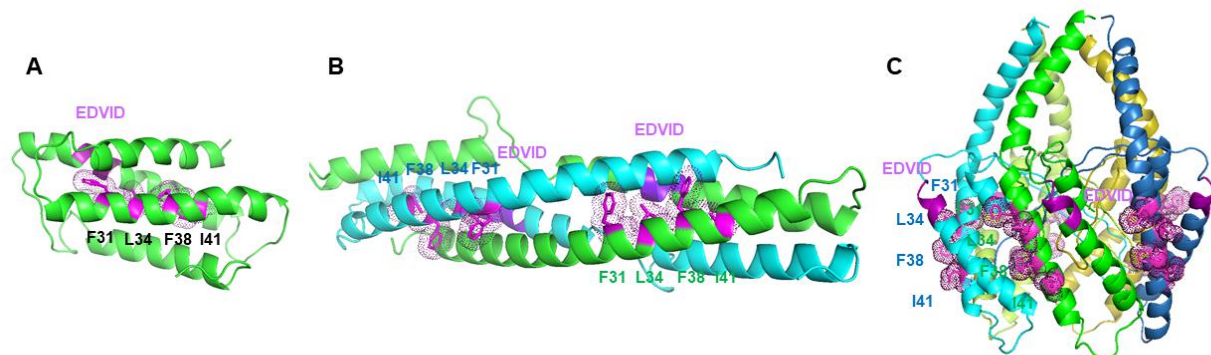
84



122 **Supplemental Figure 7. Sequence and Secondary Structure Alignment of the CC Domains**
 123 **from RB and Other NLRs Proteins.**

124 The amino acid sequences of the CC domains from RB and other NLRs, MLA10, Sr33, Rx, and
 125 ZAR1, are aligned. The heptad repeats of hydrophobic amino acids within CC domains are
 126 highlighted in yellow, the EDVID motifs in pink, and other conserved amino acids in light grey
 127 to dark corresponding to the levels of identity. The predicted α -helices of the CC domains are
 128 shown as colored cylinders.

129



130

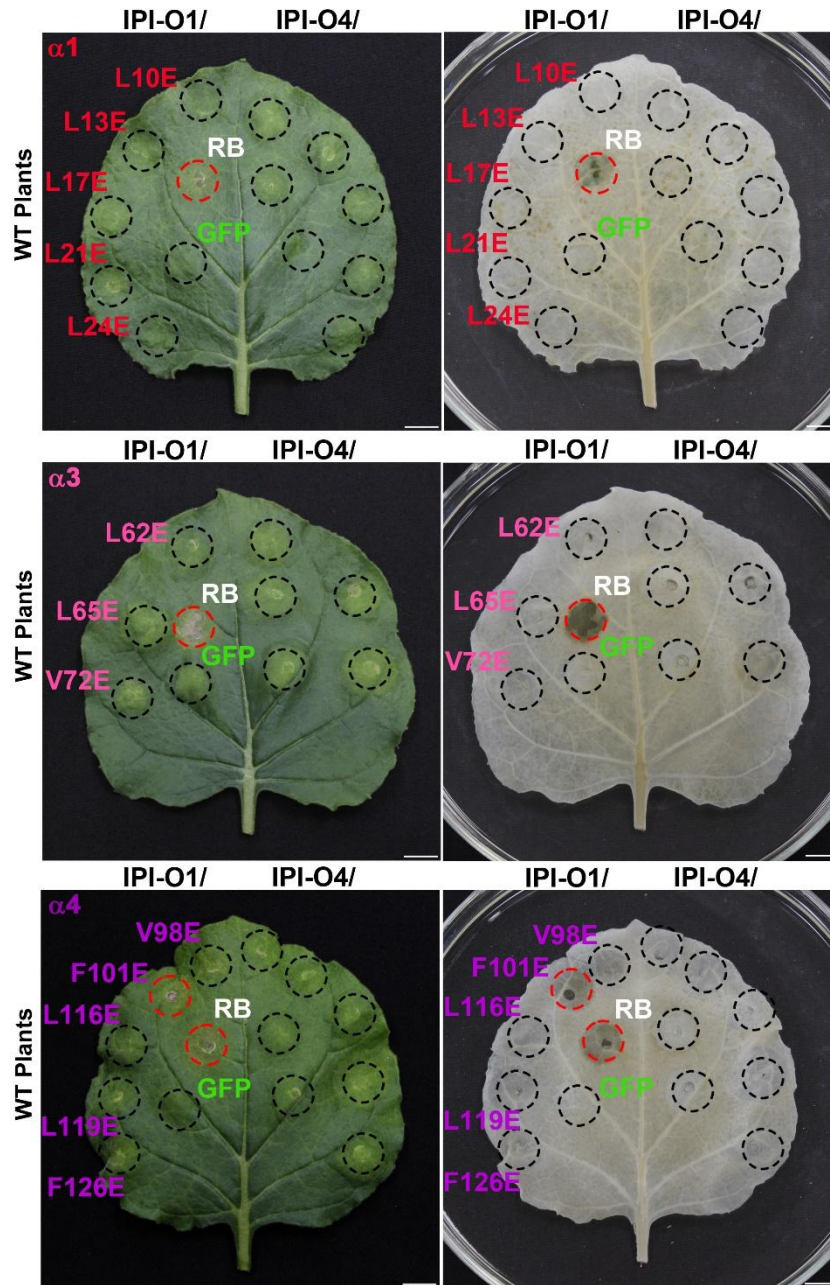
131 **Supplemental Figure 8. Ribbon Diagrams of the Predicted Monomeric, Dimeric, and**
 132 **Pentameric Structures for RB CC Domain.**

133 The predicted structures of RB CC monomer (A), dimer (B), and pentamer (C) are represented as
 134 ribbons. The four hydrophobic residues (F31, L34, F38, and I41) of the heptad repeats in the $\alpha 2$
 135 helix are highlighted in magenta. The conserved EDVID (DDILD in RB) motif is highlighted in
 136 purple. In the dimeric structure, the two monomers are shown in green and cyan. The four
 137 hydrophobic residues (F31, L34, F38, and I41) are located on the same side of the RB CC dimer.

138

139

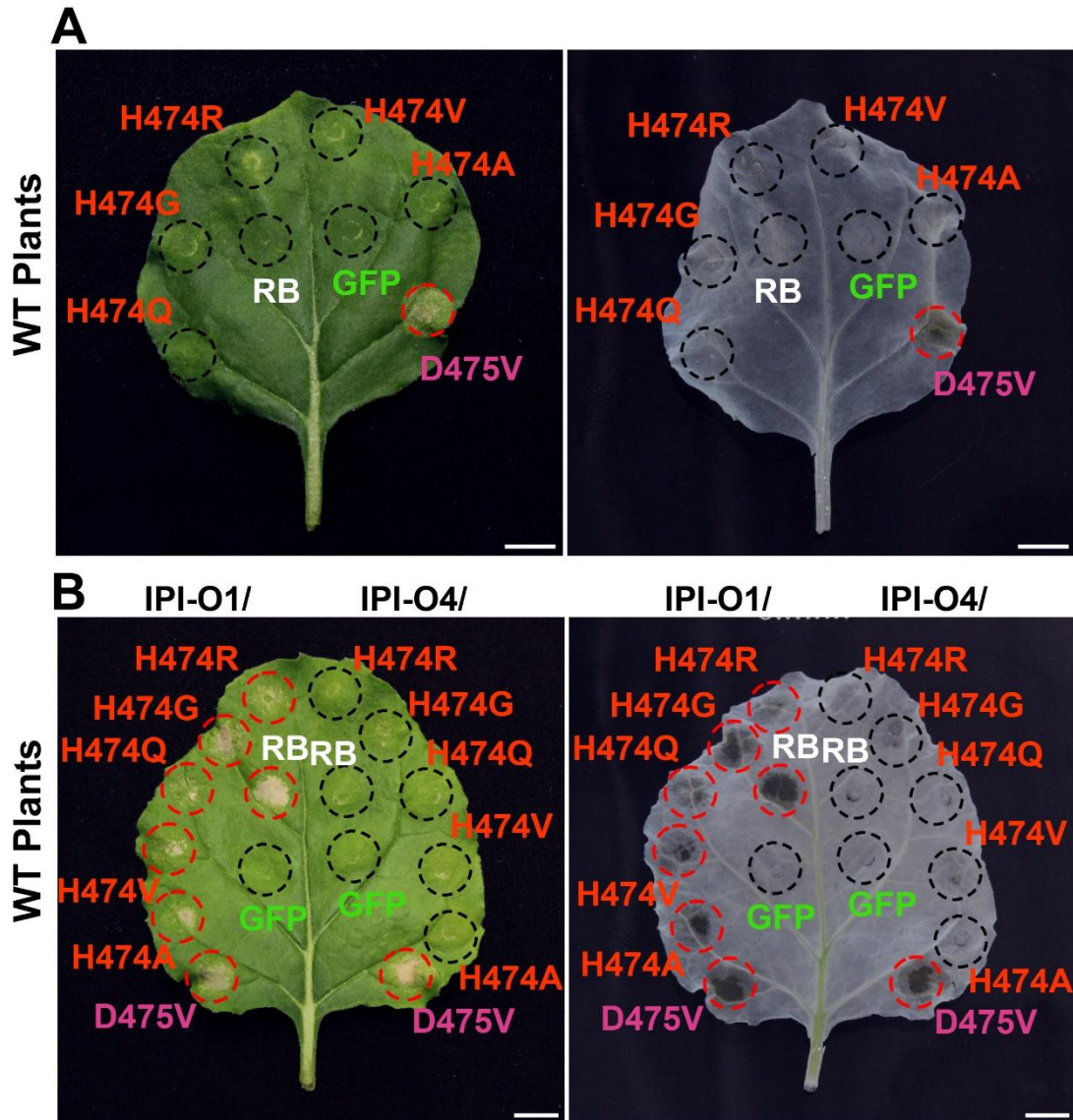
140



141

142 **Supplemental Figure 9. Mutations in the Heptad Repeats of RB Abolish Its Function.**

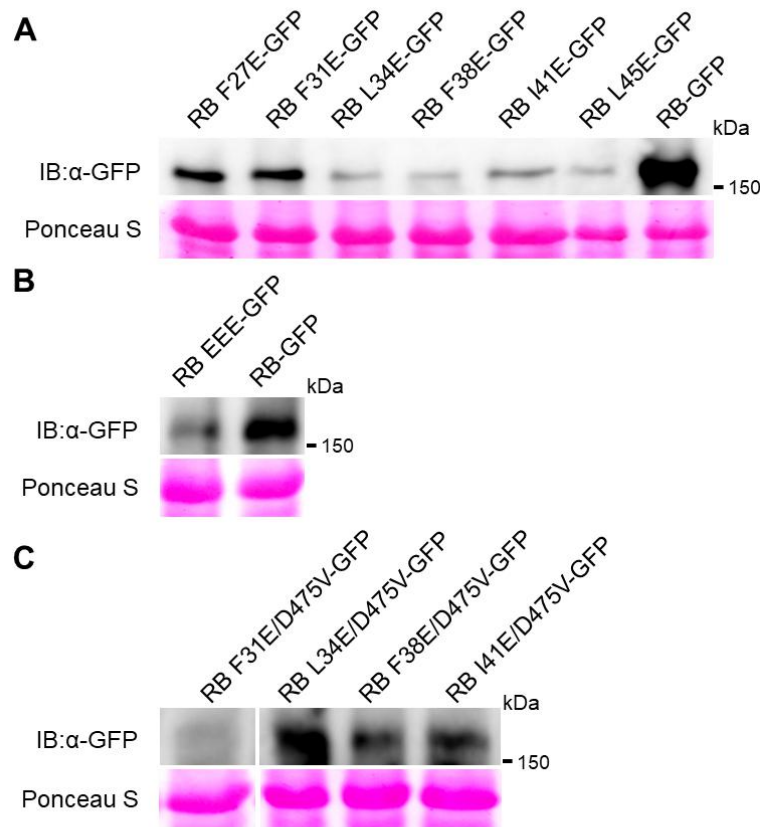
143 RB and its variants carrying mutations in the heptad repeats from the predicted $\alpha 1$, $\alpha 3$, and $\alpha 4$
 144 helices were each co-expressed with IPI-O1 or IPI-O4 in *N. benthamiana*. Cell death induced at
 145 48 hpi was visualized before (left) and after ethanol destaining (right). Infiltrated area is shown
 146 by a black circle and HR by a red circle. Scale bars represent 1 cm. The experiments were
 147 repeated six times with similar results.



148

149 **Supplemental Figure 10. Cell Death-Inducing Activities of RB MHD Mutants.**

150 (A) Cell death mediated by the RB MHD mutants in the absence of effectors. The indicated RB
 151 MHD variants were each expressed in *N. benthamiana*. (B) Cell death mediated by the RB MHD
 152 mutants in the presence of effectors. RB variants harboring mutations in the MHD motif were
 153 co-expressed with Myc-IPI-O1 or Myc-IPI-O4 in *N. benthamiana*. Cell death induced at 48 hpi
 154 was visualized before (left) and after ethanol destaining (right). Infiltrated area is shown by a
 155 black circle and HR by a red circle. Scale bars represent 1 cm. The experiments were repeated
 156 six times with similar results.



157

158 **Supplemental Figure 11. Western Blot Detection of the RB Variant Fusion Proteins.**

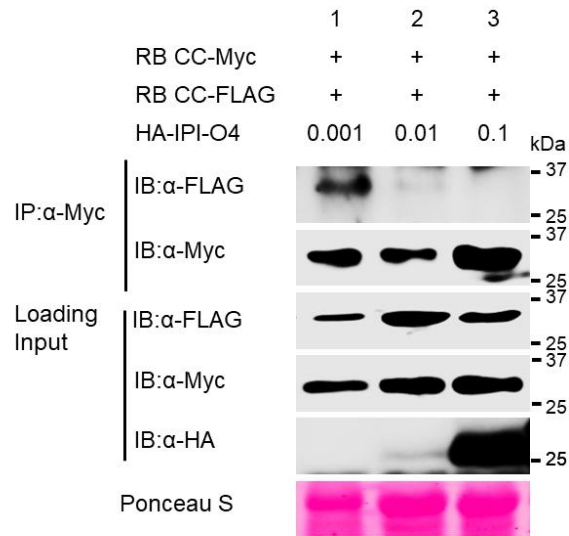
159 The GFP-tagged RB variants carrying mutations in the heptad repeats from the second α -helix
 160 (A), the F31E/L34E/I41E triple mutant (RB EEE) (B), or the autoactive D475V mutation in the
 161 MHD motif in combination with mutations in the heptad repeats of RB CC (C) were each
 162 expressed in *N. benthamiana*. The RB variant fusion proteins were extracted from leaves
 163 collected at 36 hpi and detected by Western blotting with an anti-GFP antibody. Ponceau S
 164 staining of immunoblots served as loading controls.

165

166

167

168



169

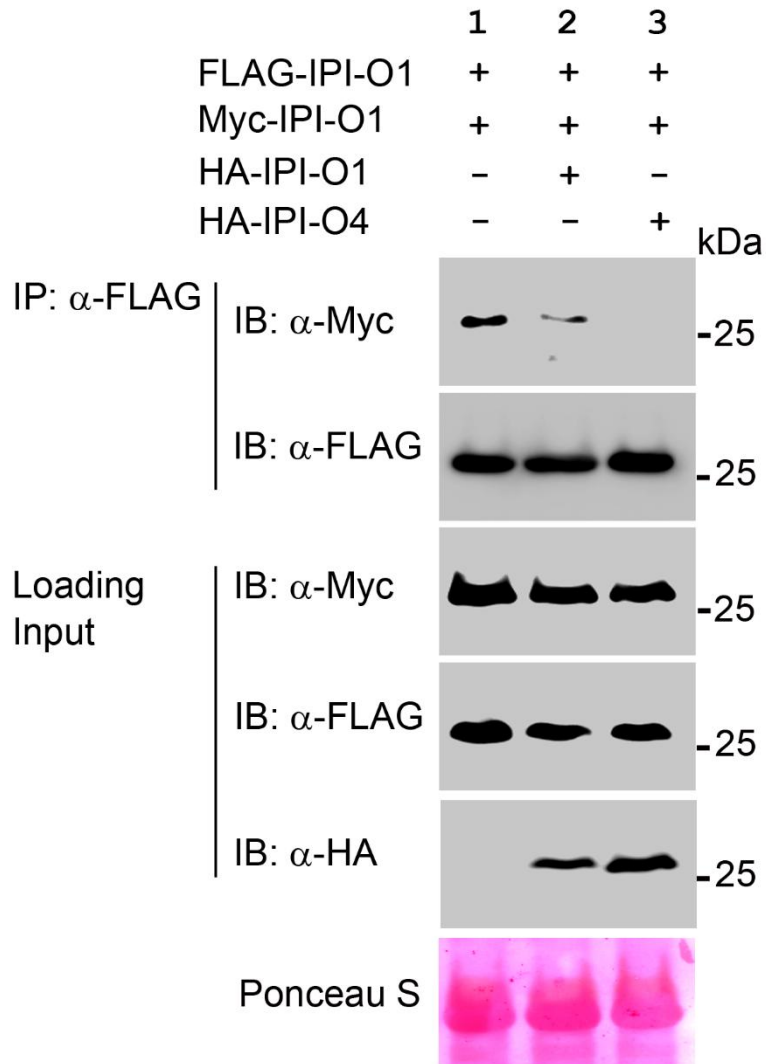
170 **Supplemental Figure 12. Disruptive Effect of IPI-O4 on the RB CC Self-Association**
 171 **Positively Correlated with the IPI-O4 Expression Level.**

172 Total proteins were extracted from *N. benthamiana* plants expressing RB CC-3×FLAG and RB
 173 CC-4 × Myc together with 3 × HA-tagged IPI-O4 at an OD₆₀₀ of 0.001, 0.01, or 0.1.
 174 Immunoprecipitation was carried out with an anti-Myc antibody, and immunoblots were probed
 175 with anti-Myc, anti-FLAG, or anti-HA antibodies. Ponceau S staining of immunoblots served as
 176 loading controls. The experiments were repeated twice with similar results.

177

178

179



180

181 **Supplemental Figure 13. Self-Association of IPI-O1 Is Perturbed by IPI-O4 *In Planta*.**

182 Total proteins were extracted from *N. benthamiana* plants expressing 3×FLAG-IPI-O1 and
 183 4×Myc-IPI-O1 together with 3×HA-tagged IPI-O1 or IPI-O4. Immunoprecipitation was carried
 184 out with anti-FLAG M2 magnetic beads, and immunoblots were probed with anti-Myc, anti-
 185 FLAG, or anti-HA antibodies. Ponceau S staining of immunoblots served as loading controls.
 186 The experiments were repeated twice with similar results.

187

188

189 **Supplemental Table 1. Oligonucleotide Sequences for Site-Directed Mutagenesis and**
190 **Plasmid Construction.**

191 Supplemental Table 1 was submitted in an Excel file.

192

193

194

195

196

197

198

199

200

201

202

203

204

205

206

207

208

209

210

211

212

213

214

215

216

217